10^{th} International Conference on Fracture Mechanics of Concrete and Concrete Structures
FraMCoS-X
G. Pijaudier-Cabot, P. Grassl and C. La Borderie (Eds)
https://doi.org/10.21012/FC10.238262

PREDICTING THE PERMEABILITY AND RELATIVE PERMEABILITY OF CONCRETE

LIONEL ECAY, DAVID GREGOIRE, AND GILLES PIJAUDIER-CABOT

E2S UPPA, Université de Pau et des Pays de l'Adour
Anglet, France
e-mail: Lionel.Ecay@univ-pau.fr
David.Gregoire@univ-pau.fr
Gilles.Pijaudier-Cabot@univ-pau.fr

Key words: permeability, unsaturated porous media, pore size distribution

Abstract. France has today reassessed the safety level of its power plants due to the Fukushima incident. The duration of the cooling system breakdown urged the industry to consider a much longer worst case scenario than was done before. The time frame for the 'severe' accident subsequently went up from 24h to two weeks. This, in turn, called for an extensive study of creep and vapour transport issues that had previously been left aside. This was the objective of the MACENA project, which aims at evaluating the tightness of a containment vessel under extreme conditions, namely a 5 bar water vapour pressure and 180C temperature during two weeks. Among the scientific issues involved in this problem, the intrinsic permeability of concrete, its relative permeability to vapour and to water and their subsequent evolution upon damage are the subject of this contribution. Our analysis starts from the work of Khaddour et al. on the impact of damage on both intrinsic and apparent permeability with the help of a random hierarchical model based on the pore size distribution of the material. This model yielded good results in terms of the evolution of permeability with damage. Here, we extend this model to the description of multiphase fluid flow. Modifications of the above-mentioned random hierarchical model involve a set of rules that capture the effect of condensation as described by Kelvin's law. In addition, the capillary assembling process is modified in order to better account for the influence of capillaries of very small diameter, which had no importance on the prediction of the intrinsic permeability but have a strong influence on the relative permeability to vapour. Segments of capillaries of small diameter are redistributed in downstream ends of the bundle according to a probability distribution that has the same shape as the pore size distribution. The extended model is shown to provide rather accurate prediction of relative permeability for a wide range of geomaterials (from mortar to tight and permeable rocks).

1 INTRODUCTION

The Fukushima-Dachi catastrophe stressed the utmost importance of prestressed reinforced concrete containment vessels in the event of a nuclear accident. The prolonged primary cooling system failure that followed the earthquake and tsunami that struck the area showed that there was a possibility for a scenario in which it was impossible to secure the power plant in a reasonable amount of time. This realization prompted EDF to revise its worst-case scenario upwards, from a few hours of primary cooling circuit breakdown to two full weeks. Such a dramatic time-scale change induces non negligible shifting of physical properties considered to be constant during a short accident (e.g.

wall saturation profile), and also brings into consideration creep issues previously left aside. For these reasons, EDF decided to start the "**MA**trise du **C**onfinement d'une **EN**ceinte en **A**ccident" (**MACENA**) project, which is aimed at assessing the tightness of containment vessels under severe accident conditions. The thermo-hygro-mechanical loading considered in this project comprises a 180C temperature, a 5 bar pressure and a 100% Relative Humidity level for two weeks. Under these conditions, the mass transport properties of concrete, considered as a non saturated porous material need to be assessed and models for the evaluation of the relative permeability of concrete to vapour and liquid water, and their evolution upon damage, need to be devised.

2 INTRINSIC PERMEABILITY

Modeling of the transport properties of porous materials has long been a subject of interest for many applications, and several theories have been discussed. The most accurate way of calculating transport properties in a porous material would be to numerically simulate a fluid flow in a 3D pore network obtained from direct sample observation. Although imaging techniques have advanced greatly in the last decades, the resolution attainable through 3D imaging is still in the micrometer region, while a significant portion of cementitious material porosity is located below that threshold. This leaves 2D imaging as the only option for observation at smaller scales, but then again recreating a Representative-Elementary-Volume-scale (REV) 3D pore network from 2D imaging is not direct. This is why, when dealing with porous materials, resorting to indirect characterization is a widely spread strategy. Considering the range of pore sizes we need to take into account to assess the porosity of cementitious materials accurately, an option is Mercury Intrusion Porosimetry (MIP), which gives access to the Pore Size Distribution (PSD) of the material, from mesopores up to microcracks.

Various efforts have been made to predict permeability with the help of capillary bundle models derived from MIP information. Kozeny [13] and Carman [1] proposed the simplest form of law by identifying a single hydraulic diameter and considering the entire porosity of the material to be made of parallel capillaries of this diameter. Garcia-Bengochea et al. [3] proposed that the parallel bundle be composed of capillaries of different diameters according to the void fraction of each pore size from the PSD measurements, which yielded better results than the single diameter approach. Different authors also proposed taking into account some form of interaction between parallel pores, or even creating pores with variable diameter. The model that we will address here is a capillary bundle arranged in a hierarchical MIP-consistant way – that is from the largest pore diameter to the smallest one, developed by Khaddour et al. [9, 12].

2.1 Random Hierarchical Bundle Model

This model was initially developed with two main objectives in mind: the first one was that the model be analytical and have no fitting parameters in order to be fully predictive, and the second that the model be able to handle a gradually damaging material (although restricted to the pre-peak regime). The network we aim at creating is a combination of parallel capillary fibers. It focuses on staying true to the MIP's philosophy, in that the capillaries we generate go from large to small diameters, in the same manner that MIP works by sequentially pushing mercury into ever smaller pores. Pore class total lengths are computed from the PSD and randomly discretized into small segments. From there on, each pore is assigned a probability of either creating a new assembly site (a new capillary fiber), or connecting randomly to any available existing one (figure 1). A segment of any given pore diameter can only be placed after a segment of larger diameter. Once an assembly site has reached the material's length – which is chosen to be the sample volume's cubic root – , its flow properties are computed and the global permeability is updated; then a new pore seg-

ment is picked and placed the same way. Once a certain convergence criterion on permeability is met, any remaining available sites are sequentially brought to completion, and when that is done, any remaining pore classes are set up into a parallel single-diameter-capillary bundle.

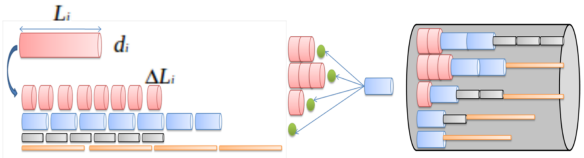

Figure 1: Pore discretization and rearrangement.

Fluid flow is described at both micro- and macro-scales, the combination of which makes it possible to retrieve macroscopic physical properties such as permeability while refining the microscopic physics involved. Micro-scale flow is computed as a combination of a viscous Poiseuille flow (Eq. 1) with a Knudsen molecular diffusion (Eq. 2).

$$Q_{Poiseuille} = \frac{\pi d^4}{256\mu}\frac{P_1^2 - P_2^2}{L_c P_2} \tag{1}$$

$$Q_{Knudsen} = \frac{\pi d^3}{12 L_c}\sqrt{\frac{8RT}{\pi M}}\frac{P_1 - P_2}{P_2} \tag{2}$$

The diffusion phenomenon combines with the existing viscous flow – as is shown on figure 2 –, increasing the overall flow when using gases for permeability measurements. The molecular diffusion depends on gas properties and pressure, while what we want to assess is the material's intrinsic permeability, which depends solely on its pore structure. This pressure dependance led Klinkenberg [8] to devise an approach for estimating intrinsic permeability from a series of flow measurements at different entry pressures: as it increases, the Knudsen proportion in the overall flow decreases. Plotted against the inverse mean pressure, the permeability can be fitted through a linear regression, yielding both the intrinsic permeability as the y-intersect and the Klinkenberg coefficient as the slope, which is a characteristic of the pore network in the material.

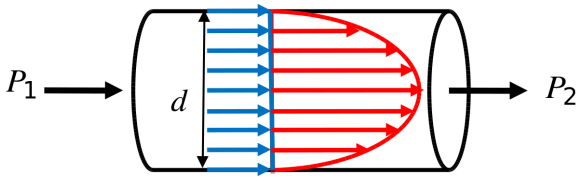

Figure 2: Velocity profile.

Meanwhile, macro-scale flow is described with a classical Darcy equation, and equating it with the sum micro-scale flows yields an explicit analytical equation for apparent permeability (Eq. 3):

$$K_a = \frac{\mu L_e}{S}\sum_{i=1}^{N_s}\frac{1}{\sum_{j=1}^{m(i)}\frac{1}{\frac{\pi d_j^4}{L_j}\left[\frac{1}{128\mu}+\frac{1}{12 d_j}\sqrt{\frac{8RT}{\pi M}}\left(\frac{1}{P_{mj}}\right)\right]}} \tag{3}$$

which is of the Klinkenberg's equation form: $K_a = K_{in}\left(1 + \frac{\beta}{P_m}\right)$.

Before discussing , the main results obtained with this model, it must be remembered that the purpose of the Random Hierarchical Bundle Model is to set the scene for statistical analyses, which implies that repeating the calculations on several capillary bundles is absolutely crucial. In the following, each result is the average of several realisations (at least 5 to 10).

2.2 Intrinsic permeability and evolution with damage

The model is first confronted to several experimental pore size distributions obtained on mortar specimens that have been loaded in uniaxial compression, up to several levels so that damage occurs. Upon unloading, damage measured as the resulting degradation of the unloading stiffness has been recorded, prior to the measurement of the pore size distribution with the help of mercury intrusion. Details of this study can be found in Ref. [12].

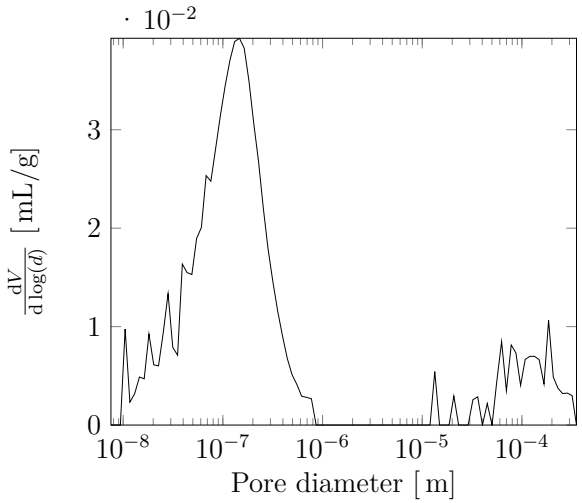

Figure 3: Pore size distribution of mortar before damage.

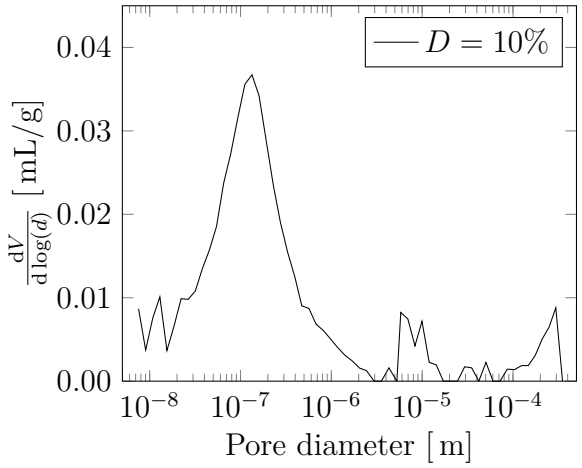

Figure 4: Pore size distribution of mortar after damage damage.

Intrinsic and apparent permeability calculations were performed on undamaged mortar samples (Fig. 6) and on four others of the same batch at different damage levels ($D = 2.5, 7, 10$ and 12%). The pore size distributions of these last samples is shown in Fig. 4. The evolution of the intrinsic permeability with damage is shown in Fig. 5 and the evolution of the Klinkenberg coefficient is plotted on Fig. 6.

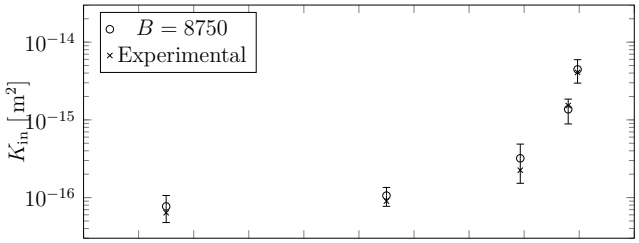

Figure 5: Evolution of the intrinsic permeability with damage - comparison with experiments.

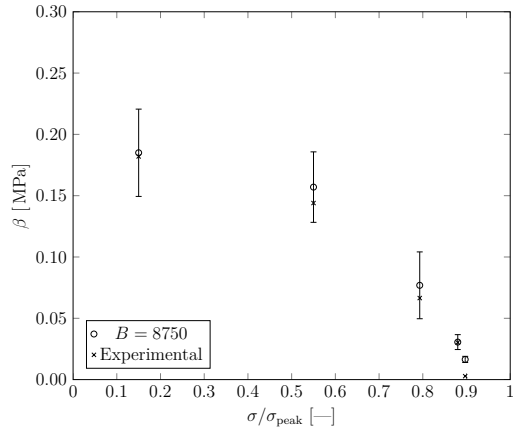

Figure 6: Evolution of Klinkenberg coefficient with damage - comparison with experiments.

The permeability of specimens measured prior to any damage is well within the standard deviation produced by the hierarchical model. Upon damage, the predicted evolutions of both the intrinsic permeability and of the Klinkenberg coefficient are also in agreement with experiments.

The hierarchical model has been also model was confronted to several other materials in an effort to assess its range of applicability. Among these we find:

- three different concretes reported in Refs. [2, 7] by Chen et al. and Kallel respectively. The first one uses CEM I Portland cement, the second one uses CEM V, highly concentrated in fly ashes and blast-furnace slag. The third one is the concrete used in the MACENA project. The PSD of the CEM I specimens is shown in Fig. 7 and the PSD of the MACENA concrete

is shown in Fig. 8. The parameters in the hierarchical model are the same as those used for the calculations on mortar.

- Sandstone tested by Osselin et al. [14] (Fig. 9). The same adaptation used for the above material has been implemented in the calculations because the signal at the wide end of the range exhibits no noise at all and it is expected to be physically meaningful..

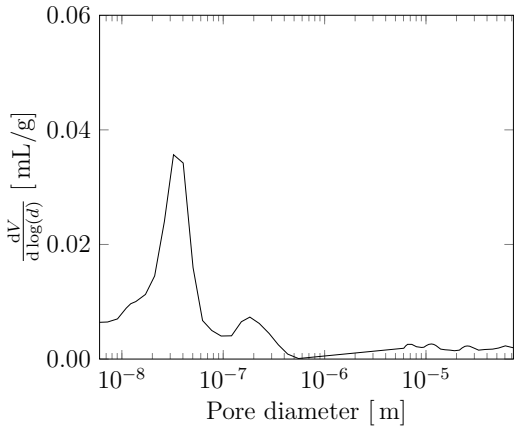

Figure 7: Pore size distribution for CEM I concrete specimens.

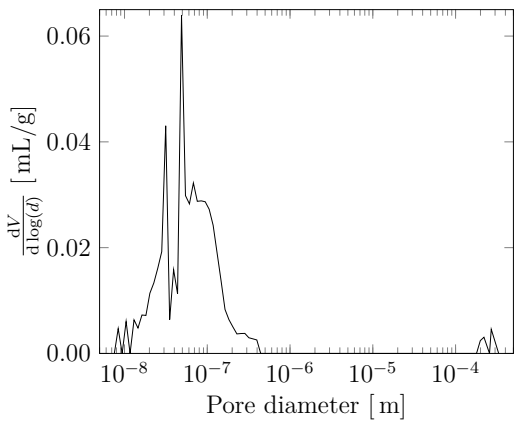

Figure 8: Pore size distribution for MACENA concrete.

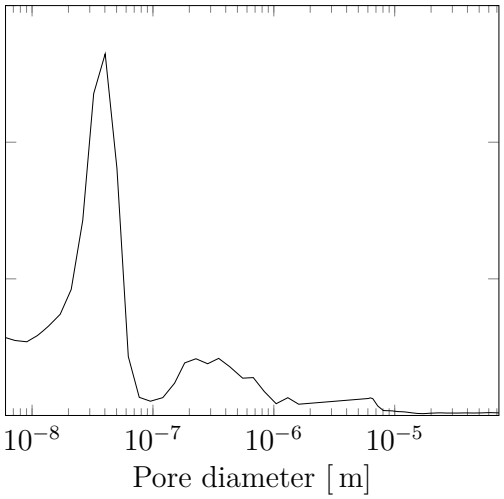

Figure 9: Pore size distribution for sandstone specimens (after [14]).

The intrinsic permeabilities obtained for each material are reported, along with experimental data in table 1.

Table 1: Experimental and model intrinsic permeabilities

Specimen	$K_{\text{exp.}}$ [m^2]	K_{model} [m^2]
CEM I	$3.5.10^{-18}$	$[0.7–1.3].10^{-17}$
CEM V	$3.4.10^{-18}$	$[6.4–7.2].10^{-17}$
MACENA concrete	$4.1.10^{-17}$	$[4.1–6.6].10^{-17}$
Sandstone	$1.5..10^{-13}$	$[1.0–1.8].10^{-13}$

As can be seen, the model stands rather well across a wide range of materials spanning four orders of magnitude in permeability, which is a good validation point. Chen's concretes are of particular interest here because they are cementitious materials as well and fall within the same permeability range as those of Khaddour's mortars. While in the right order of magnitude, the model's accuracy in this case is slightly lower compared to the results on mortar. This discrepancy could probably come from the fact that the PSD datasets provided by Chen et al. were not obtained using the same MIP apparatus. Indeed, one parameter involved in the random hierarchical bundle model is related to the accuracy of the measurement technique under low mercury pressure, which exhibits a lot of noise usu-

ally [10, 12]. This parameter may vary from one device to the other.

3 RELATIVE PERMEABILITY

Up until then, the model only considered a porous medium fully saturated with a single fluid, be it either gas or liquid. The reality of porous media is almost always in-between, though, with the pore space invaded by a mixture of two phases, one of which is wetting while the other is non-wetting. In cementitious materials for instance the pore space starts out fully water-saturated when it is cast. Then over time, pore-space water put in contact with an outer atmosphere at a relative humidity lower than 100% gradually evaporates, leading to a non-linear saturation profile inside the material. It is therefore critical to be able to determine the wetting- and non-wetting-phase permeabilities in order to properly assess global flows for both phases. We are going to expand the model in order for it to take varying saturation levels into account.

3.1 Modification of the hierarchical model and redistributive approach

The fundamental notion that needs to be kept in mind is the definition of two variables of interest that will be used henceforth, which are called *relative permeabilities*. They are defined for each phase as the phase-permeability to intrinsic permeability ratio, which means they are comprised between 0 and 1.

$$k_{\mathrm{rg}} = \frac{K_{\mathrm{g}}}{K_{\mathrm{in}}} \tag{4}$$

$$k_{\mathrm{rl}} = \frac{K_{\mathrm{l}}}{K_{\mathrm{in}}} \tag{5}$$

where subscript r stands for relative and subscripts g and l stand for gas and liquid, respectively, although their more general definition would be wetting and non-wetting.

Consider that the medium starts out with its pore space fully saturated with non-wetting fluid, more specifically gas in our case. As gas pressure rises, it eventually reaches a point where it condensates due to confinement within the pore space, as expressed in Kelvin's equation:

$$\ln(RH) = \frac{-2\gamma v_m}{rRT} \tag{6}$$

where RH denotes relative humidity $p_{\mathrm{vapor}}/p_{\mathrm{saturation}}$, $2/r$ stand for a meniscus curvature (supposed hemispherical here because of perfect wetting and cylindrical pores are assumed), γ stands for surface tension, v_m stands for the liquid's molar volume, R is the ideal gas constant and T the temperature. While hysteretic behaviour is experienced during wetting-drying experiments on $RH - Sr$ graphs, the fact that the model uses actual water content saturation Sr means that the hysteretic link with relative humidity RH is of no direct concern. Indeed this hysteresis remains in the $RH - Sr$ space and does not impact relative permeability, as demonstrated by [2]. Because of the way the pore assembly within this model is built, we have a general pore profile consisting of several segments of varying diameters, assembled from wide to narrow. Because of equation 6, this means that water vapor will first condensate in the last segment of each assembly, the narrower one. From this point out, we can classify three different situations:

- if no segment is clogged due to condensation, the pore assembly is fully vapour-saturated in its intrinsic permeability is added to the overall gas permeability;
- if at least one but not all segments is clogged due to gas condensation, the assembly participates neither to gas nor to liquid permeability. Also, we do not consider the possibility of the liquid plug being pushed out of the pore due to the pressure gradient. This could be implemented at a later stage, but whether that is relevant is open for discussion. Indeed, the idealised view of a pore network assembled from larger to smaller pores, while consistent with MIP, is not topologically representative of the actual material, and applying this kind of physics to it might

not be sensible. Furthermore, one could argue that in the actual material it is more than likely that the smallest pores will be connected at both ends to larger ones and experience smaller pressure differentials than the global one applied to the sample. In this case, little to no plug pushing could occur anyway;

- and if all segments are condensated with water, the assembly is supposed to contribute to overall water permeability.

These three situations are represented on figure 10.

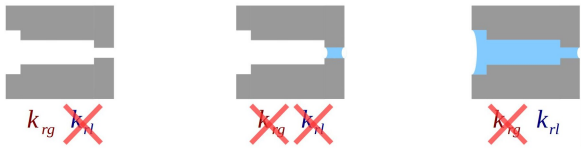

Figure 10: Pore states.

This whole process ties relative humidity to saturation levels through the material's PSD, as all pores of any given size are considered to condensate at the same time. Thus a saturation level and its corresponding relative permeabilities can be computed for every pore size. However, the above rules are not sufficient in order to provide meaningful predictions of the relative permeability gas which is severely overestimated. Smaller pores – which account for a limited part of the overall permeability when the pore network is saturated with a single fluid – do not have as strong an impact on the decrease of relative permeability to gas as they should when they become saturated.

One possible explanation is that given their significant volume and very small diameters, these pores ought to be connected to others, what is not captured in the hierarchical model which assemble them into a bundle of capillary fibers of constant diameter. The underlying principle of the modified model is that small pores should represent a higher proportion of narrow pore throats in the model than they previously did because of their high volume and spatial distribution. We set out to recreate pore throats by placing tiny increments of these narrower pores at the end of the existing assembly. These increments should be small enough so that their combined volume is a negligible fraction of their class' total volume and that permeability is only slightly affected if at all. What will henceforth be referred to as *redistributive approach* is the fact of placing short small pore segments downstream of existing capillaries in order to recreate narrow pore throats.

For this concept to work, length ΔL of the adjoined pore segment j has to be computed by defining a permeability drop for the assembly. This is done by first calculating its permeability without segment j and then postulating a dropped permeability that remains a relatively high fraction of the original. We estimate a 1% drop to be acceptable as it falls well within the variability range of the model itself.

The initial assembly's permeability is given in equation 7 and can be compared to its after-redistribution counterpart 8. Once permeability drop η is defined, unknown length ΔL of pore segment j needed to reach the target is written as equation 9:

$$K_{\text{in,before}} = \frac{\pi L_s}{128 S_s} \frac{1}{\sum_{i=1}^{m} \left(\frac{L_i}{d_i^4} \right)} \tag{7}$$

$$K_{\text{in,after}} = \frac{\pi (L_s + \Delta L)}{128 S_s} \frac{1}{\sum_{i=1}^{m} \left(\frac{L_i}{d_i^4} \right) + \frac{\Delta L}{d_p^4}} \tag{8}$$

$$\Delta L = \frac{\eta \sum_{i=1}^{m} \left(\frac{L_i}{d_i^4} \right)}{\frac{1-\eta}{d_p^4} - \frac{1}{L_s} \sum_{i=1}^{m} \left(\frac{L_i}{d_i^4} \right)} \tag{9}$$

where η is the permeability drop, ΔL the adjoined pore length and L_s the sample length.

Now that determining the pore length to be adjoined is cleared, a strategy has to be put in

motion in order to decide which pore size will be used. In an effort to keep the random nature of the model, pore diameter determination will be done randomly and for every capillary. At this stage, the principal element still to be determined is a transfer function that will translate randomly sorted numbers between 0 and 1 into diameters.

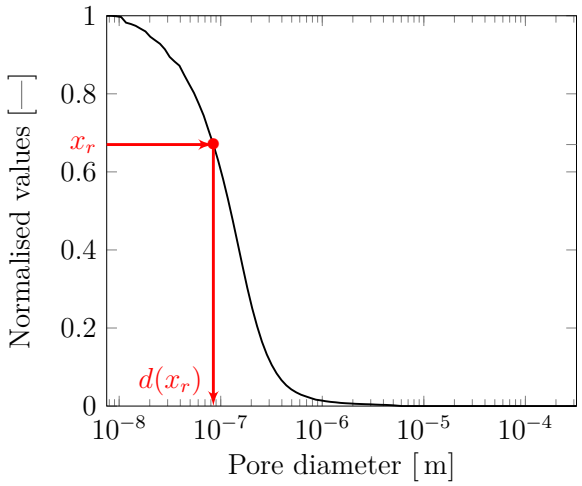

Figure 11: Transfer function – Normalised cumulative pore volume.

This function should follow a few guidelines, first of which is the absence of fitting parameters. Indeed the existing model came to a certain degree of predictivity, which we would not want to disrupt more than necessary. It should also ideally hold some form of physical meaning. Based on these general aims, we decided to use the normalised cumulative pore volume curve as a transfer function for the redistribution process. The function focuses on redistributing smaller pores in order to account for their effect on relative permeabilities and the whole process needs to remain true to the initial hierarchical approach by which pore assemblies systematically go from wider to narrower. Also, the equiprobability of sorting any random number between 0 and 1 means that adjoined diameter sorting probability density follows to some extent the pore size distribution. An example of such a function is shown on figure 11. Determination of redistributed pore diameters occurs by sorting random number x_r, reporting it on the y-axis, reporting to the curve and reading the corresponding x-axis value as the diameter, which is also shown on Fig. 11.

Once the initial hierarchical bundle has been formed, iterations start covering each capillary assembly. Determination of redistributed pore diameters is performed by sorting random number x_r, reporting it on the y-axis, reporting to the curve and reading the corresponding x-axis value as the diameter, which is also shown on Fig. 11. Whenever randomly sorted pore diameter $d(x_r)$ is bigger than exit diameter $d(j)$ of current assembly j no redistribution is made.

3.2 Results

We first compare a concrete sample from the MACENA project whose transport properties were obtained by [7] and which was characterised via MIP, yielding the PSD shown in figure 8. Results for gas and liquid relative permeabilities are plotted against experimental data on figure 12. The sample was tested under load inside a climatic chamber at different temperatures for this purpose.

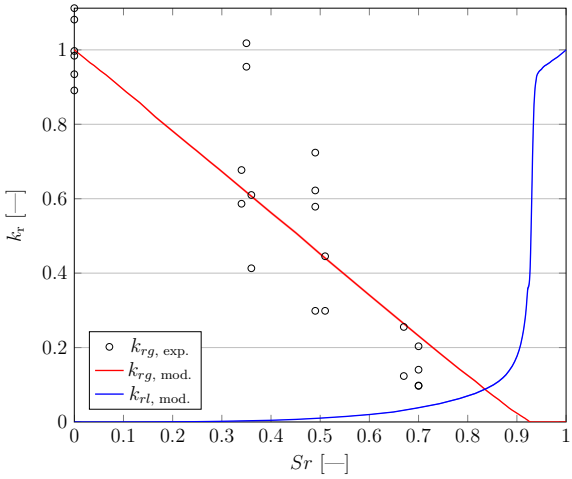

Figure 12: Relative permeability for MACENA concrete.

While relative permeabilities comply well with experimental data and intrinsic permeability is successfully predicted, the wide dispersion of relative permeability measurements is worth noting, and might mean that this cannot be taken as clear evidence to the model's validity. Figure 13 shows the model predictions

obtained for the CEM I concrete whose PSD is provided in Fig. 7. Relative permeabilities are predicted with a relatively correct accuracy. Gas relative permeability k_{rg} plot needs a slightly greater curvature, meaning that smaller pores should have an even stronger impact on permeability than they currently do in order to properly assess experimental data.

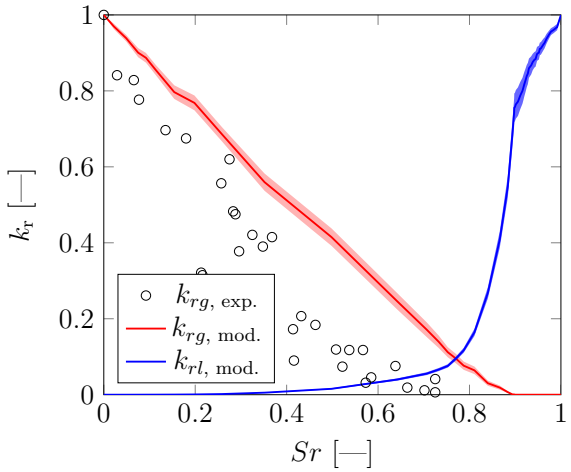

Figure 13: Relative permeability for CEM I concrete.

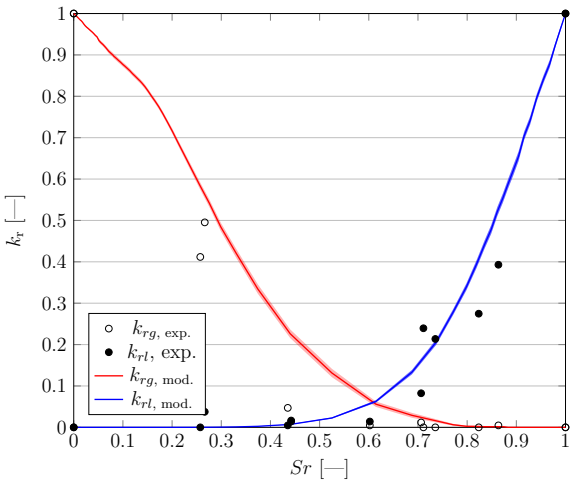

Figure 14: Relative permeability for sandstone.

In order to explore the predicting capabilities of the model, we have also considered two types of rocks. The first one is the sandstone whose pore size distribution is provided in Fig. 9. Experimental and predicted relative permeabilities appear on figure 14. With this simple monodisperse strongly peaked pore size distribution the model was able to capture both the intrinsic permeability – although it is four orders of magnitude higher than for concrete and mortar – and liquid and gas relative permeabilities as well, which fall spot on experimental measurements.

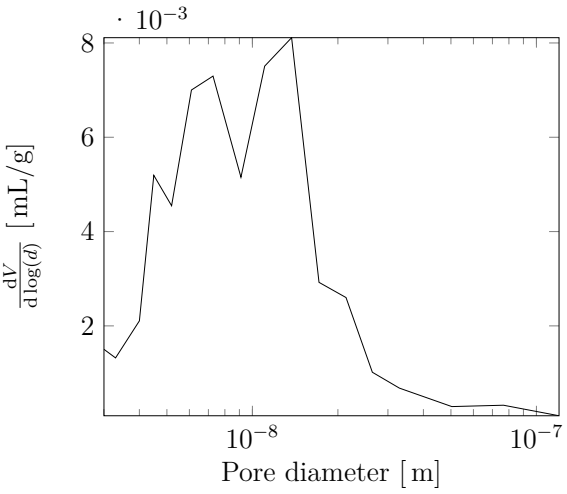

Figure 15: Pore size distribution of clay.

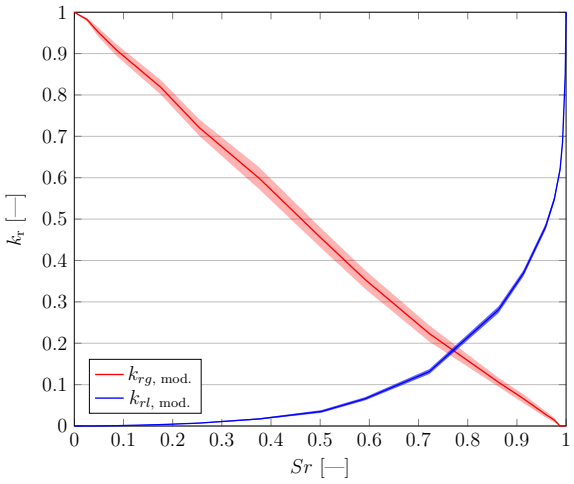

Figure 16: Relative permeability for clay.

We will now investigate the model's behaviour when confronted with a very low permeability material, in this specific case a clay dating back to Callovo-Oxfordian times. This rock is being studied as a geological repository for long-term nuclear waste storage. Its relative permeabilities are not available in the literature

yet. Its pore size distribution is presented on figure 15. its experimental intrinsic permeability is $4.2.10^{-19}m^2$, close to the the model prediction ($3.6.10^{-19}m^2$). Relative permeabilities are reported in Fig. 16.

4 Closure

In this paper, a model aimed at predicting the intrinsic and relative permeability of a porous material has been presented. The model uses as input the pore size distribution of the material, measured according to mercury intrusion porosimetry. It is based on a random hierarchical assembly of capillary segments, hence it is basically a one-dimensionnal model that should yield an isotropic permeability tensor.

First, the model has been compared to experiments performed on mortar undergoing states of increasing damage in uniaxial compression. Without any calibration parameter (except those related to the apparatus from which the PSD is obtained), the model is capable of providing a very accurate prediction of the intrinsic permeability of the material, and of the Klinkenberg's coefficient as well when permeability to gas is considered. In addition, different materials with permeability ranging over 4 orders of magnitude have been considered, hereby demonstrating that the model provides consistent results.

Second, we have discussed the introduction of partial saturation in the above Random Hierarchical Bundle Model. In order to do so have assumed a completely dry initial state and sequential condensation in all pore classes as vapor pressure gradually increases, following Kelvin's equation. This rule being set, the model needed to be further enhanced. As Poiseuille flow depends on the capillary diameter's fourth power, smaller pores have no weight whatsoever on permeability, and their saturation does not impact relative gas permeability anywhere near as much as it should. A process was therefore devised to take the effect of small pores on permeability upon saturation. Supposing that what is observed is the direct consequence of the presence of pore throats throughout the porous material that are gradually closed off upon condensation, this new redistributive approach aims at simulating their presence in the model's random and parallel bundles after their initial generation. This approach was confronted to various sets of experimental data. Overall, the extended hierarchical model provides rather good predictions of the relative permeability to water and vapour.

Finally, it should be pointed that intrinsically, the effect of pressure and temperature on permeability is included in this random hierarchical model. Such comparisons are the subject of further research efforts.

Acknowledgements

This sudy has been performed with the financial support of ANR through the PIA MACENA project.

5 REFERENCES

REFERENCES

[1] Carman P.C. 1937. Fluid flow through granular beds, Transactions-Institution of Chemical Engineeres, Vol. 15, PP. 150-166.

[2] Chen, W., Liu, J., Skoczylas, F., Davy, C., Bourbon, X., Talandier, J. 2012. Water retention and gas relative permeability of two industrial concretes, Cement and Concrete Res., 42, pp. 1001-1013.

[3] Garcia-Bengochea, I., Altschaeffl, A.G., Lovell, C.W. 1979. Pore distribution and permeability of silty clays, Journal of the Geotechnical Engineering Division, Vol. 105, pp. 839-856.

[4] Ecay, L. 2018, Concrete transfer properties evolution and nuclear vessel tightness assessment during an accident, *Ph.D. Dissertation*, Université de Pau et des Pays de l'Adour.

[5] Jason, L. 2004. Relation endommagement perméabilité pour les bétons: application aux calculs de structures, *Ph.D. Dissertation*, Ecole Centrale de Nantes.

[6] Jason, L., Pijaudier-Cabot, G., Ghavamian, S. Huerta, A. 2007. Hydraulic behaviour of a representative structural volume for containment buildings, Nuclear engineering and design, Vol. 237, pp. 1259-1274.

[7] Kallel, H. 2016, Influence de la température et de l'hygrométrie sur le comportement instantané du béton, *Ph.D. Dissertation*, Université de Pau et des Pays de l'Adour.

[8] Klinkenberg L.J. 1941. The permeability of porous media to liquids and gases, *Drilling and production practice*, American Petroleum Institute.

[9] Khaddour, F., Gregoire, D., Pijaudier-Cabot, G. 2014. Computing permeation properties of mortar from pore size distributions, *Computational modelling of concrete structures*, CRC press, Vol. 1, pp. 405-414.

[10] Khaddour, F. 2015. Amélioration de la production de gaz des Tight Gas Reservoirs, *Ph.D. Dissertation*, Université de Pau et des Pays de l'Adour.

[11] Khaddour, F., Gregoire, D., and Pijaudier-Cabot, G. 2015. Capillary bundle model for the computation of the apparent permeability from pore size distributions, European journal of environmental and civil engineering, Vol. 19, pp. 168-183.

[12] Khaddour, F., Gregoire, D., and Pijaudier-Cabot, G. 2018. A Hierarchical Model for the Computation of Permeation Properties of Porous Materials and their Enhancement due to Microcracks, J. Engrg. Mech. ASCE, Vol. 144, 04017160.

[13] Kozeny, J. 1927. Über kapillare Leitung des Wassers im Boden:(Aufstieg, Versickerung und Anwendung auf die Bewässerung), Hölder-Pichler-Tempsky.

[14] Osselin, F., Fabbri, A., Fen-Chong, T. Pereira, J.M., Lassin, A., Dangla, P. 2015. Experimental investigation of the influence of supercritical state on the relative permeability of Vosges sandstone, Comptes Rendus Mécanique, Vol. 343, pp. 495-502.

[15] Van Genuchten, M.T. 1980. A closed-form equation for predicting the hydraulic conductivity of unsaturated soils, Soil science society of America journal, Vol. 44, pp. 892-898.